

## **CORONAL MASS EJECTION INITIATION: On the nature of the Flux Cancellation Model**

T. Amari

*CNRS, Centre de Physique Théorique de l'Ecole Polytechnique, F-91128 Palaiseau Cedex,  
France*

amari@cpht.polytechnique.fr

J.-J. Aly

*AIM - Unité Mixte de Recherche CEA - CNRS - Université Paris VII - UMR n<sup>o</sup> 7158,  
Centre d'Etudes de Saclay, F-91191 Gif sur Yvette Cedex, France*

Z. Mikic and J. Linker

*Predictive Science Inc., San Diego, CA 92121, USA*

### **ABSTRACT**

We consider a three-dimensional bipolar force-free magnetic field with non zero magnetic helicity, occupying a half-space, and study the problem of its evolution driven by an imposed photospheric flux decrease. For this specific setting of the Flux Cancellation Model describing coronal mass ejections occurring in active regions, we address the issues of the physical meaning of flux decrease, of the influence on field evolution of the size of the domain over which this decrease is imposed, and of the existence of an energetic criterion characterizing the possible onset of disruption of the configuration. We show that: (1) The imposed flux disappearance can be interpreted in terms of transport of positive and negative fluxes towards the inversion line, where they get annihilated. (2) For the particular case actually computed, in which the initial state is quite sheared, the formation of a twisted flux rope and the subsequent global disruption of the configuration are obtained when the flux has decreased by only a modest amount over a limited part of the whole active region. (3) The disruption is produced when the magnetic energy becomes of the order of the decreasing energy of a semi-open field, and then before reaching the energy of the associated fully open field. This suggests that the mechanism leading to the disruption is nonequilibrium as in the case where flux is imposed to decrease over the whole region.

*Subject headings:* magnetohydrodynamics (MHD) — stars: coronae — stars: magnetic field — stars: flare — Sun: coronal mass ejections (CMEs) — Sun: flares

## 1. INTRODUCTION

Magnetic flux cancellation (FC) is a well documented solar photospheric phenomenon (Welsch 2006) which plays the key role in the Flux Cancellation Model (FCM). FCM has been introduced initially to explain flux rope and prominence formation (van Ballegoijen & Martens 1989), and applied later on for modelling large scale eruptive events such as Coronal Mass Ejections (CMEs) occurring in active regions (see, e.g., Forbes et al. (2006) for a review). In the latter context, it has been actually developed in two settings differing from each other essentially by the way FC is introduced: FC is either taken to be a physical consequence of the photospheric turbulent diffusion, or just imposed as a time dependent boundary condition describing a decrease of the flux according to some prescribed law. In the former case, first considered in Amari et al. (2003b) and later on in Yeates & Mackay (2009), Yeates et al. (2010), and Aulanier et al. (2010), the dispersive effect of the turbulence on the flux of an active region leads to the bringing together on the inversion line of some amounts of flux of both polarities, which thus get annihilated by small scale mixing. This type of FCM is of course particularly relevant when one wants to explain the CMEs which occur during the decaying phase of an active region. The second type of FC implementation was first applied to study the possible disruption of 2D bipolar configurations (Forbes & Priest 1995), and later on of 3D bipolar configurations (Amari et al. 2000; Linker et al. 2001) and 3D quadrupolar ones (Amari et al. 2007).

Although previous works have led to a good understanding of FCM in the “flux decreasing setting”, there are many points which are still unclear. (1) The disappearance of flux on the boundary is imposed as a mere mathematical boundary condition, and doubts have been sometimes expressed about the possibility that it be related to some physical process. To keep viable this setting of the FCM, we thus need to provide a physical interpretation of flux decrease compatible with the observations. For instance, the latter show FC to be often associated to the mutual annihilation of opposite polarity flux elements brought into contact by photospheric motions, and an interpretation in terms of flux transport and annihilation on an inversion line would be certainly adequate. An other possibility would be to interpret FC in terms of emergence through the photosphere of either an U-loop or a bipolar loop, flux decrease occurring in the latter case once the magnetic axis has started emerging (see Fan (2001) and Amari et al. (2005) for simulations, and López Fuentes et al. (2000)

for observations). (2) Previously, flux decrease has been imposed to occur over the whole active region, or at least the whole central bipolar part in the case of a quadrupolar region (Amari et al. 2007). In many cases, however, one may expect FC to occur over only a small part of the region, and the question arises of the possibility of still triggering a disruption in that case. (3) If a disruption actually occurs, we have finally to address the question of the nature of its trigger. Basically, there are three possible mechanisms (Amari & Aly 2009): Non Equilibrium (NE), Quasi Non Equilibrium (QNE), meaning equilibrium too far to be accessible, and Unstable Equilibrium (UE). For instance, we found QNE to be responsible for the transition to very fast expansion exhibited by a flux rope twisted by boundary motions (Amari et al. 1996). In the case of a bipolar (Amari et al. 2000) or quadrupolar (Amari et al. 2007) configuration submitted to FC, on the contrary, we found NE to be at the origin of the eruption. This conclusion was established by showing that the magnetic energy of the system exceeds the energy of the associated totally open field in the former case, and the energy of a partially open field (having its open lines being connected only to the part of the boundary where strong currents once developed) in the latter one. Then we should look in particular for the existence of a similar energy criterion if a disruption occurs as a consequence of partial FC.

The aim of the present Letter is to address these important issues in the case where the initial configuration is force-free and has a nonzero magnetic helicity. Physically, such a field may be thought of either resulting from the emergence of a twisted flux rope (TFR) through the photosphere, or being the remnant of a configuration which has previously generated an eruptive event without fully relaxing to a potential field (Amari & Luciani 1999), or to be produced by photospheric twisting motions. It is worth insisting on the fact that the evolutions we consider are only driven by FC, in opposition to some other works (van Ballegooijen et al. 2000; Aulanier et al. 2010) in which FC is applied along with shearing motions.

## 2. MODEL AND INITIAL CONFIGURATION

In our numerical model, the “coronal half-space”  $\{z > 0\}$  above an active region is represented by a large computational box  $\Omega_h = [-20, 20] \times [-20, 20] \times [0, 40]$ , equipped with a non uniform mesh of 141x131x121 nodes. The used physical quantities are dimensionless. In particular the Alfvén crossing time  $\tau_A$  is taken as the time unit.  $\Omega_h$  contains a perfectly conducting low density plasma with an embedded magnetic field  $\mathbf{B}$ . For  $t \geq 0$ , this system is brought into a two-stages MHD evolution: a preliminary stage, not claimed to represent an actual coronal evolution, which produces a force-free equilibrium with a nonzero helicity,

and a second stage, which is the physically relevant one, in which the previous field is taken as the initial state of a FC driven evolution. Both phases are controlled by imposing on the “photospheric” boundary  $S_h$  of  $\Omega_h$  (on which  $z = 0$ ) the tangential component of the electric field,  $\mathbf{E}_s$ , a procedure which is known from our previous works to lead to a well posed problem. Quite generally,  $\mathbf{E}_s$  can be Helmholtz decomposed according to

$$c\mathbf{E}_s = \nabla_s \phi + \nabla_s \psi \times \hat{\mathbf{z}}, \quad (1)$$

where  $\nabla_s = \hat{\mathbf{x}} \partial_x + \hat{\mathbf{y}} \partial_y$ , and  $\phi(x, y, t)$  and  $\psi(x, y, t)$  are solutions, respectively, of the equations  $\nabla_s^2 \phi = c \nabla_s \cdot \mathbf{E}_s$  and  $-\nabla_s^2 \psi = c \hat{\mathbf{z}} \cdot \nabla_s \times \mathbf{E}_s$ . Using Faraday law thus leads to

$$\partial_t B_z = -c \nabla \cdot (\mathbf{E}_s \times \hat{\mathbf{z}}) = \nabla_s^2 \psi. \quad (2)$$

The MHD equations are solved by our numerical algorithm (Amari et al. 1999, 1996). Small values are chosen for the dissipation coefficients:  $\nu = 10^{-2} - 10^{-3}$  for the kinematic viscosity, and  $\eta$  not larger than  $10^{-4}$  for the resistivity, giving for our mesh resolution a Lundquist number not smaller than  $10^4$ .

In the first stage, we start at  $t = 0$  from a bipolar potential magnetic field  $\mathbf{B}_\pi = \nabla V_\pi$ .  $V_\pi$  is the solution of a Dirichlet-Neuman boundary value problem for Laplace equation, in which we impose in particular the condition

$$B_{\pi z}(x, y, 0) = q(x, y) = e^{-x^2/\sigma_x^2} \left[ e^{-(y-y_c)^2/\sigma_y^2} - e^{-(y+y_c)^2/\sigma_y^2} \right] \quad (3)$$

on  $S_h$ , with  $y_c = -0.8$ ,  $\sigma_x = 1$ ,  $\sigma_y = 2$ . For  $0 \leq t \leq 400$ , we apply on  $S_h$ , as in Amari et al. (2003a), the tangential electric field  $\mathbf{E}_s$  associated to  $\psi = 0$  and a  $\phi$  such that  $\phi'(B_z) = B_z \Phi'(B_z)$ , with  $\Phi(B_z)$  a prescribed function. This generates slow shearing/twisting  $B_z$ -preserving ideal motions of the magnetic footpoints at the velocity  $\mathbf{v}_s = c \nabla_s \phi \times \hat{\mathbf{z}} / B_z$  (with  $\max(v_s) = 10^{-2}$ ). A neighbouring nonlinear force-free equilibrium is next reached by performing for  $400 \leq t \leq 800 = t_0$  a viscous relaxation phase during which  $\phi = \psi = 0$  and  $B_z$  is still conserved on  $S_h$ . As shown on Figure 1, this equilibrium is sheared along the neutral line, and because of twist, it exhibits away from that line the presence of strong electric currents correlated with the typical sigmoidal structure. It is worth noticing that, for this equilibrium, we have  $\text{supp}(FFF) \subset \text{supp}(B_z)$ , where  $\text{supp}(FFF)$  and  $\text{supp}(B_z)$  denote the regions where, respectively, electric currents and  $B_z$  are strong enough.

### 3. PARTIAL FLUX CANCELLATION

For driving the FC phase, we fix  $\mathbf{E}_s$  on  $S_h$  by setting  $\phi(x, y, t) = 0$  and by taking  $\psi$  to satisfy  $\nabla_s^2 \psi(x, y, t) = -\mu \zeta(y) B_z(x, y, 0, t_0) = -\mu \zeta(y) q(x, y)$  on  $S_h$ , with  $\mu = 10^{-2} > 0$ ,

and  $\zeta(y) = [1 + \tanh[(y_1 - y)/d]][1 + \tanh[(y - y_0)/d]]/4$ .  $\zeta$  exhibits a "plateau" of height 1 in the interval  $[y_0, y_1]$  and falls down to zero in a layer of thickness  $d$ . It is used as a mask controlling the size of the cancellation support,  $supp(FC)$ . We use here the particular values  $y_0 = -0.5, y_1 = 0.5, d = 0.1$ , whence  $supp(FC) \subset supp(FFF) \subset supp(B_z)$  as the width of each Gaussian polarity is approximately equal to 2 and decreases at a slower rate. The case considered in Amari et al. (2000) (where FC is enforced over the whole bipolar region) corresponds to  $\zeta = 1$ . Using Eq. (2), we have  $\partial_t B_z(x, y, 0, t) = -\mu\zeta(y)q(x, y)$ , whence after an immediate integration

$$B_z(x, y, 0, t) = q(x, y)[1 - \mu\zeta(y)(t - t_0)]. \quad (4)$$

Then  $B_z$  suffers a linear decrease on  $S_h$ . But this does not lead to any specific problem as the reduction factor  $[1 - \mu\zeta(y)(t - t_0)] \geq 0.62 > 0$ , the FC phase being limited to a duration of about 38 (see below). All along that phase, we regularly apply viscous relaxation runs to check if a neighbouring equilibrium exists or not. We found this strategy to be more appropriate than the one used in Amari et al. (2007), where the need to effect episodic relaxations was bypassed by choosing a much smaller value of  $\mu$  ( $\mu = 10^{-4}$ ).

As stated in Section 1, it is crucial for the validity of the model that the mathematically imposed flux decrease be interpretable in physical terms. Let us show that it can be actually considered to result from the transport of opposite polarities fluxes towards the inversion line  $I$  where they annihilate indeed. In any case, we can introduce on  $S_h$  an horizontal velocity of magnetic flux transport,  $\mathbf{u}$ , by setting  $c\mathbf{E}_s + B_z\mathbf{u} \times \hat{\mathbf{z}} = 0$ . Using the Helmholtz decomposition (1) of  $c\mathbf{E}_s$  and Eq. (4), we obtain at once

$$\mathbf{u}(x, y, t) = -\nabla_s\psi(x, y)/[q(x, y)(1 - \mu\zeta(y)(t - t_0))]. \quad (5)$$

During the FC phase,  $\mathbf{u}$  appears to be just continuously rescaled by a time dependent factor on most of  $supp(FC)$ , where  $\zeta = 1$ , and to remain invariant outside  $supp(FC)$ , where  $\zeta = 0$ . Interestingly, we see that the cancellation flow support,  $supp(CF)$ , coincides approximately with  $supp(B_z)$ , and is then not reduced to  $supp(FC)$  for a localized FC. The velocity  $\mathbf{u}$  computed at some time is shown on Figure 2a, and it is clearly seen to be directed indeed towards  $I$  in a neighbourhood of that line. Note that we have removed from the plot the parts very close to  $I$  and very far from the spots, respectively, where  $u$  becomes very large. The flux  $B_z\mathbf{u}$  of  $B_z$  keeps however a finite value on  $I$ , on which  $\nabla_s\psi$  does not vanish, and the flow thus continuously advects magnetic flux onto that line, where it disappears. On the other hand, it should be noted that the velocity pattern at any other time during the FC phase is identical to the one shown on Figure 2a because of the simple scaling property proved above.

That flux decrease may be associated with flux annihilation on the inversion line  $I$  can be also simply proved in a quite general way as follows. Let us consider for a little while an

arbitrary initial distribution  $B_z(t_0)$  on  $S_h$ , and prescribe a flux decrease by setting  $\partial_t B_z = f_c(x, y, t)$ , with  $f_c \geq 0$  on  $S_h^+$ , where  $B_z > 0$  ( $f_c \leq 0$  on  $S_h^-$ , where  $B_z < 0$ ), and  $\int_{S_h} f_c ds = 0$ . We define as above the flux transport velocity  $\mathbf{u}$  by  $B_z \mathbf{u} = c \mathbf{E}_s \times \hat{\mathbf{z}} = \nabla_s \phi \times \hat{\mathbf{z}} - \nabla_s \psi$ . Then we have

$$\int_I B_z u_N dl = \int_I (\partial_t \phi - \partial_N \psi) dl = - \int_{S_h^+} f_c ds > 0, \quad (6)$$

where  $\mathbf{N}$  is the exterior normal on  $S_h$  to  $\partial S_h^+$  (and then to  $I$ ), and  $u_N = \mathbf{u} \cdot \mathbf{N}$ . For estimating the second member, we have used Gauss theorem, the equation  $\nabla_s^2 \psi = f_c$  (which results from Eq. (2)), and assumed  $\partial_N \psi$  and  $\phi$  to vanish on the far part of the boundary. We can thus conclude that, "in the mean sense", we have in a neighbourhood of  $I$  (into which  $\mathbf{N}$  has been extended)  $u_N > 0$  on the + side and  $u_N < 0$  on the – side, which corresponds indeed to a finite amount of fluxes of both signs being transported towards  $I$ , where they cancel. But of course, for arbitrary functions  $B_z(t_0)$  and  $f_c$ , and associated sinuous shape of  $I$ , we expect to have in general  $u_N < 0$  ( $u_N > 0$ ) on the + (–) side of some "little" part of  $I$ , i.e., local emergence of flux, and FC holds only globally. That this does not happen in the particular case considered in this Letter is due to the fact that we consider a configuration with antisymmetric flux distribution ( $q(x, -y) = -q(x, y)$ , whence  $I = \{y = 0\}$ ), and impose  $f_c = -\mu \zeta q$ , with  $\zeta$  symmetric ( $\zeta(-y) = \zeta(y)$ ). Finally, we note the following relation, which holds for the latter specific choice of  $f_c$ . Consider an arbitrary curve  $C$  surrounding the positive part of  $\text{supp}(FC)$ , with external normal  $\hat{\mathbf{N}}$ . Setting  $\Phi(t) = \int_{\text{supp}(FC)^+} B_z ds$  and proceeding as above, we get

$$\int_C B_z u_N dl = -d_t \Phi = \mu \int_{\text{supp}(FC)^+} \zeta q ds \simeq \mu \Phi(t_0) \quad (7)$$

Increasing the size of  $\text{supp}(FC)$  increases  $\Phi(t_0)$  and thus the mean velocity  $\langle u_N \rangle$ .

For a turbulent diffusion driven evolution (Amari et al. 2003b), the arguments above, based on our Helmholtz decomposition of  $\mathbf{E}_s$ , also apply, thus providing a formal proof that cancellation flows are associated to that process too.

#### 4. TWISTED FLUX ROPE, DISRUPTION, AND TRIGGERING MECHANISM

We now describe the evolution of the coronal field driven by FC.

(1) During a first phase, there is a transition from an arcade topology to a twisted flux rope (TFR) topology. This transition is not instantaneous. Rather we observe more

and more field lines close to  $I$  forming dips and a TFR progressively grows from those as flux is advected towards  $I$ . A coherent TFR exists at  $t = t_{FR}$ . In particular J-shape loops have "merged", generating the inverse topology characteristic of the TFR, with dips able to support prominence material, as seen on Fig. 3. Such a feature was also found in the simulations reported in Amari et al. (2000). During the transition, the mutual helicity of the two J-shape loops is converted into the TFR self-helicity.

(2) During this phase, viscous relaxation always leads to a neighbouring equilibrium. The TFR created along the neutral line grows up both laterally and vertically, as new flux participates to its structure. As expected for a system in near equilibrium (Aly 1984, 1991; Sturrock 1991), we find that  $W_\pi(t) < W(t) < W_\sigma(t)$ , where  $W(t)$  is the magnetic energy of the configuration, and  $W_\pi(t)$  and  $W_\sigma(t)$  are, respectively, the energies of the potential field  $\mathbf{B}_\pi(t)$  and the open field  $\mathbf{B}_\sigma(t)$  having the same flux distribution on  $S_h$  as  $\mathbf{B}(t)$ .  $W(t)$  and  $W_\pi(t)$  are observed to decrease slightly, while the ratio  $W(t)/W_\pi(t)$  increases (see Fig. 2b). This behaviour is expected since  $W_\pi(t)$  depends only on the photospheric flux distribution, decreasing by FC, while  $W(t)$  depends also of the volumic distribution of coronal currents. As  $W_\pi(t)$ ,  $W_\sigma(t)$  depends only on the photospheric flux distribution and decreases, but the inequality  $W_\sigma(t) > W(t)$  stays satisfied as FC has not yet been very effective.

(3) After a critical time  $t_{gd} \approx 838$ , the configuration experiences a global disruption, as shown on Figure 4, and FC is switched off. Viscous relaxation does no longer lead to an equilibrium close to  $\mathbf{B}(t)$ , and the configuration evolves dynamically towards opening (see Fig. 5). As in Amari et al. (1996, 2000, 2003a,b, 2007), opening is characterized by a transition to very fast expansion suffered by a bundle of lines, which thus close down eventually at very large distances. Along with that process, reconnection develops through the overlying arcade and a current sheet forms below, associated to dissipation. At this stage, since our results rely only on viscous relaxation, it can be either that there exists an accessible equilibrium, but that it is unstable (case UE of our classification) or that such an equilibrium does not exist (case NE of our classification). Discriminating between the two situations could be done in principle by first trying to compute force-free equilibria satisfying the boundary conditions on  $B_n$  and  $\alpha = (\nabla \times \mathbf{B})_z / B_z$  given by the evolution model before and after  $t_{gd}$ , respectively (e.g., by using the Grad-Rubin methods developed in Amari et al. (2006)), and by studying their stability when they exist. But this is a difficult task since convergence of the equilibrium algorithms might be difficult to achieve around the critical point, while testing stability requires superimposing perturbations of some types. Then, as we favor a priori NE to be responsible for the disruption, we adopt as in Amari et al. (2000, 2007) the strategy consisting to show that a necessary condition for the existence of an equilibrium ceases to be satisfied at  $t_{gd}$ .

(4) The idea is that it becomes energetically favorable for the system to open once the magnetic energy  $W(t)$  starts exceeding the energy of an accessible semi-open field  $\mathbf{B}_{SO}(t)$ . The  $\mathbf{B}_{SO}(t)$  which seems to be relevant here is defined as follows: it has all its lines connected to  $supp(SO)$  being open and all the other lines being closed. A priori  $supp(SO)$  can be reasonably defined in two different ways: it can be identified either with the part of  $S_h$  to which the fast expanding lines are connected, or with the part of  $S_h$  where the twist/shear of the initial force-free field is concentrated. Happily, however, the two definitions select the same region  $supp(SO)$ . We thus estimate  $W_{SO}(t)$  by equating it to the energy of the potential field  $\mathbf{B}'_{\pi}(t)$  satisfying  $B'_{\pi z} = |q_0|$  on  $supp(SO)$  and  $B'_{\pi z} = q_0$  on  $S_h \setminus supp(SO)$ . As guessed, it appears that the transition to NE occurs indeed when  $W_{SO}(t)$ , which decreases faster than  $W(t)$ , becomes comparable to the latter. In fact Figure 2b shows that, while  $W(t)/W_{\pi}(t)$  increases,  $W_{SO}(t)/W_{\pi}(t)$  decreases, and the two curves cross for  $t \simeq t_{gd}$ . From this point, any attempt to find a neighbouring equilibrium fails and the configuration experiences a major disruption as shown on Figure 5.

We note finally that the amount of cancelled flux at  $t_{gd}$  is about 6%, a small value compared to the 30% found in Amari et al. (2000) and even below the 9% found in the quadrupolar case in Amari et al. (2007). Note that the initial states considered in these previous works were also quite highly sheared. We can thus state that a small amount of FC is sufficient to trigger a large disruption. But we do not pretend in any case that the 6% value is general. Depending on the initial state, a higher or lower amount of partial cancellation may be needed for a large disruption to be produced. And for low shear initial states, it is even possible that only a confined eruption be obtained as in Amari et al. (2003b).

TA thanks G. Aulanier for discussion. We acknowledge support from NASA's Sun-Earth Connection Theory Program, NASA's STEREO/SECCHI Consortium and Centre National d'Etudes Spatiales. The numerical simulations performed in this paper have been done on the NEC SX8 supercomputer of the Institute I.D.R.I.S of the Centre National de la Recherche Scientifique.

## REFERENCES

Aly, J. J. 1984, ApJ, 283, 349

—. 1991, ApJ, 375, L61

Amari, T. & Aly, J. 2009, in IAU Symposium, Vol. 257, IAU Symposium, ed. N. Gopalswamy & D. F. Webb, 211–222



- Amari, T., Aly, J. J., Mikic, Z., & Linker, J. 2007, *ApJ*, 671, L189
- Amari, T., Boulmezaoud, T. Z., & Aly, J. J. 2006, *A&A*, 446, 691
- Amari, T. & Luciani, J. F. 1999, *ApJ*, 515, L81
- Amari, T., Luciani, J. F., & Aly, J. J. 2005, *ApJ*, 629, L37
- Amari, T., Luciani, J. F., Aly, J. J., Mikic, Z., & Linker, J. 2003a, *ApJ*, 585, 1073
- , 2003b, *ApJ*, 595, 1231
- Amari, T., Luciani, J. F., Aly, J. J., & Tagger, M. 1996, *ApJ*, 466, L39
- Amari, T., Luciani, J. F., & Joly, P. 1999, *SIAM J. Sci. Comput.*, 21, No. 3, 970
- Amari, T., Luciani, J. F., Mikic, Z., & Linker, J. 2000, *ApJ*, 529, 529
- Aulanier, G., Török, T., Démoulin, P., & DeLuca, E. E. 2010, *ApJ*, 708, 314
- Fan, Y. 2001, *ApJ*, 554, L111
- Forbes, T. G. & Priest, E. R. 1995, *ApJ*, 446, 377
- Forbes, T. G., Linker, J. A., Chen, J., Cid, C., Kóta, J., Lee, M. A., Mann, G., Mikić, Z., Potgieter, M. S., Schmidt, J. M., Siscoe, G. L., Vainio, R., Antiochos, S. K., & Riley, P. 2006, *Space Sci. Rev.*, 123, 251
- Linker, J. A., Lionello, R., Mikić, Z., & Amari, T. 2001, *J. Geophys. Res.*, 106, 25165
- López Fuentes, M. C., Demoulin, P., Mandrini, C. H., & van Driel-Gesztelyi, L. 2000, *ApJ*, 544, 540
- Sturrock, P. A. 1991, *ApJ*, 380, 655
- van Ballegooijen, A. A. & Martens, P. C. H. 1989, *ApJ*, 343, 971
- van Ballegooijen, A. A., Priest, E. R., & Mackay, D. H. 2000, *ApJ*, 539, 983
- Welsch, B. T. 2006, *ApJ*, 638, 1101
- Yeates, A. R., Attrill, G. D. R., Nandy, D., Mackay, D. H., Martens, P. C. H., & van Ballegooijen, A. A. 2010, *ApJ*, 709, 1238
- Yeates, A. R. & Mackay, D. H. 2009, *ApJ*, 699, 1024

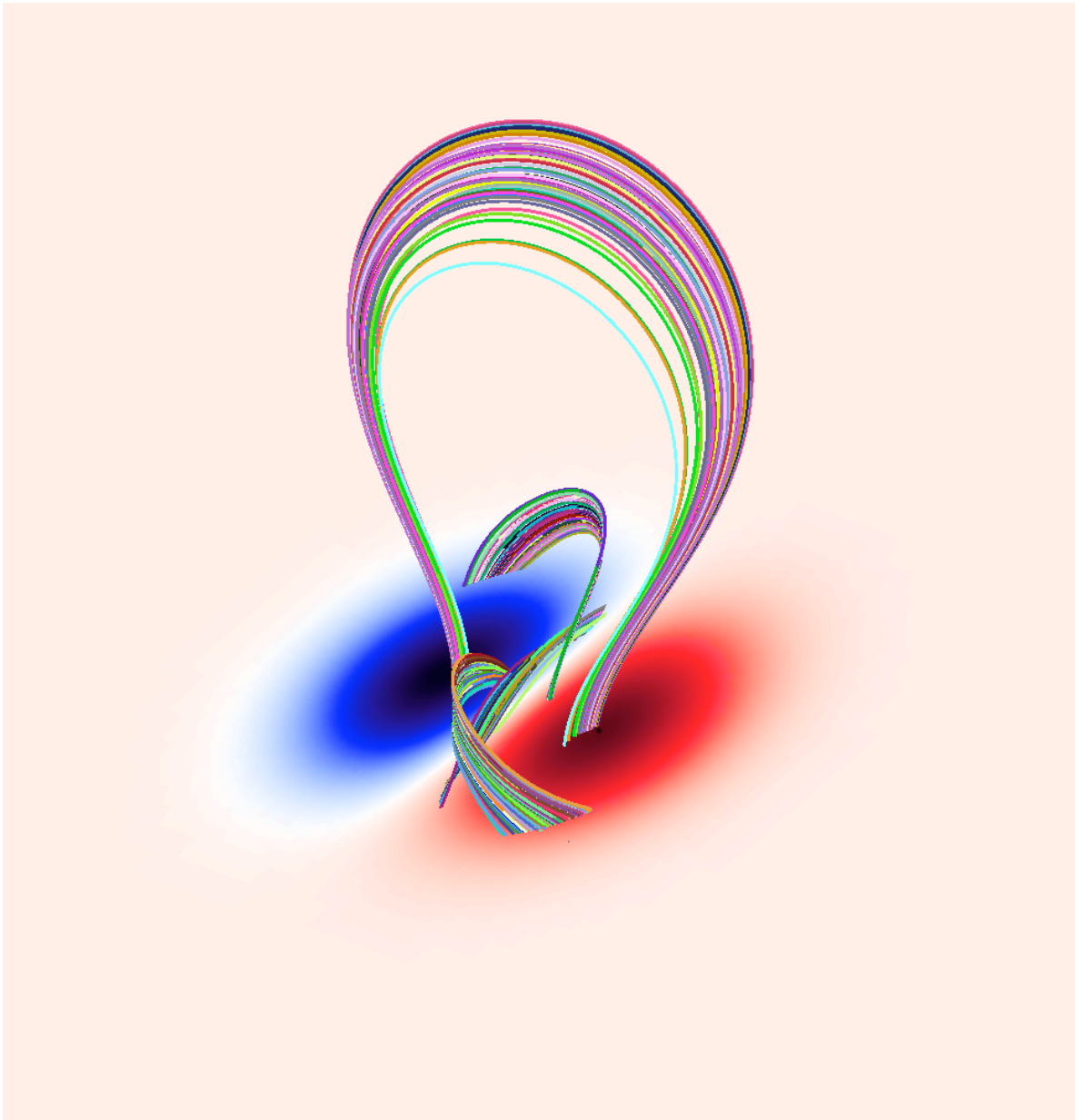


Fig. 1.— Selected field lines of the initial force-free configuration reached after a shearing-twisting phase followed by a viscous relaxation. Strong shear is accumulated along the neutral line.

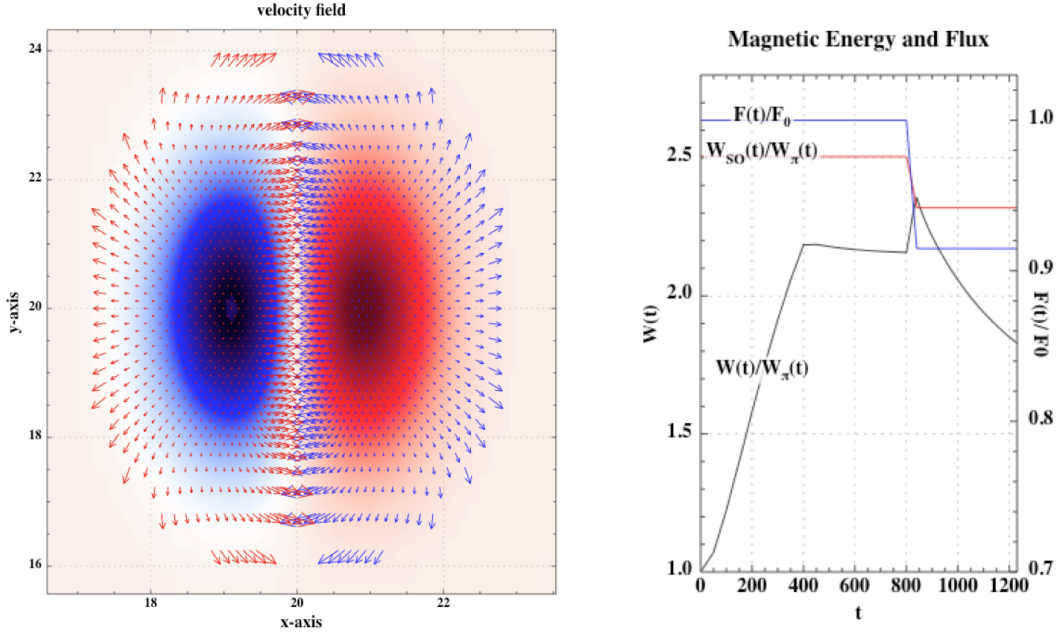


Fig. 2.— (a) Plot of the velocity field associated with the imposed flux decrease. This flow is indeed a cancellation flow as it brings flux elements of opposite polarities into contact along the inversion line, where they get annihilated. (b) Time variations of some important quantities during the phase of twisting by boundary motions of the initial potential field ( $0 \leq t \leq 400$ ), the phase of viscous relaxation ( $400 \leq t \leq 800$ ), the phase of FC ( $800 \leq t \leq 838$ ), and the nonequilibrium phase ( $838 \leq t$ ). Are represented the normalised unsigned flux  $F(t)/F_0$  through  $S_h$ , the free magnetic energy measure  $W(t)/W_{\pi}(t)$  (which increases during the FC phase), and the free energy measure  $W_{SO}(t)/W_{\pi}(t)$  (which decreases during FC phase) of a semi-open field which has all its open lines originating from the region on which the shear/twist is distributed. The last two curves intersect at some critical time, corresponding to a FC of less than 6%, beyond which the global disruption occurs.

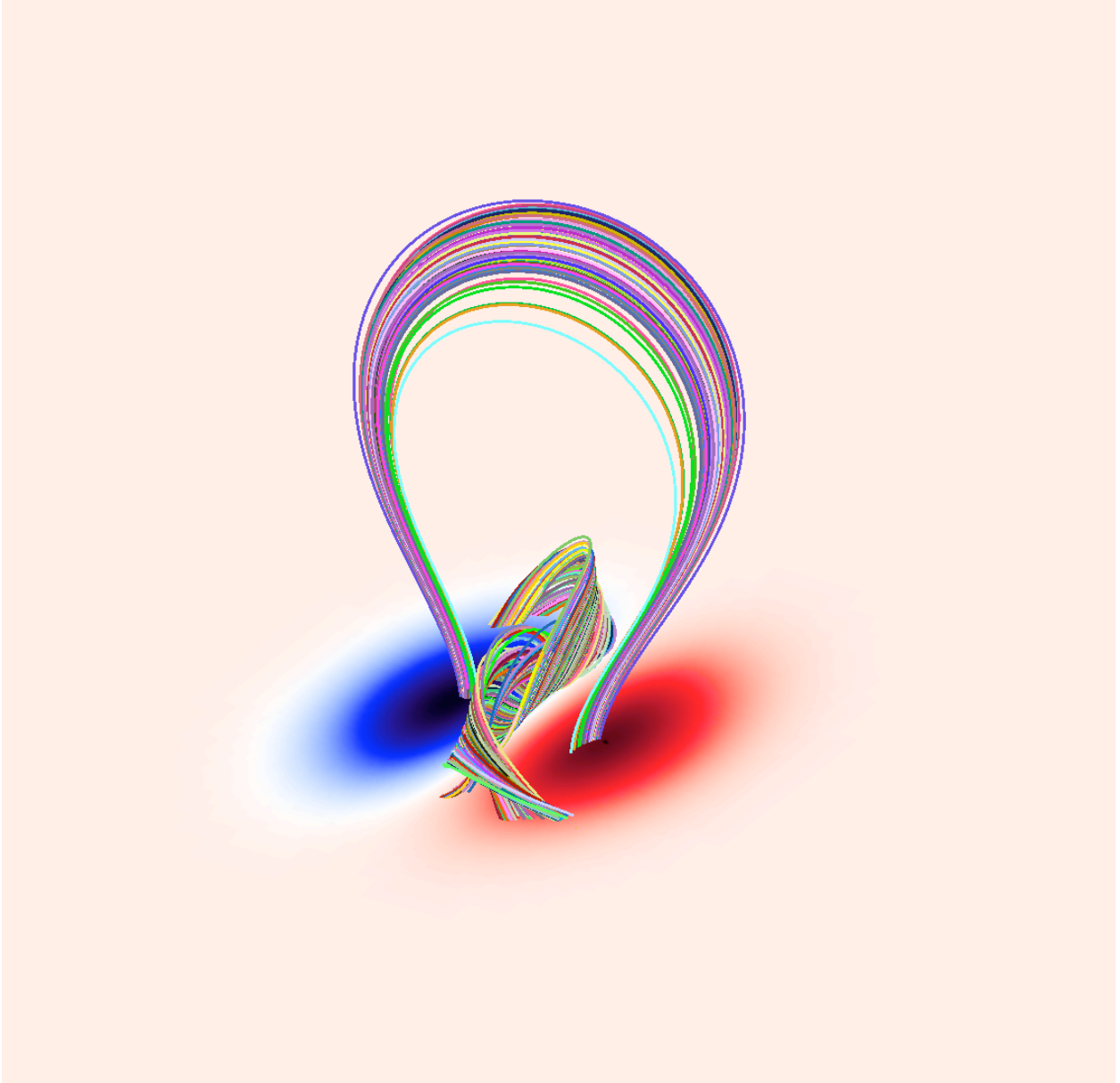


Fig. 3.— Selected field lines of the equilibrium configuration obtained at  $t = 820$ , i.e., during the phase of localised flux cancellation. A TFR exhibiting dips favourable to the support of cool material has formed from the two J-shape loops seen on Figure1.

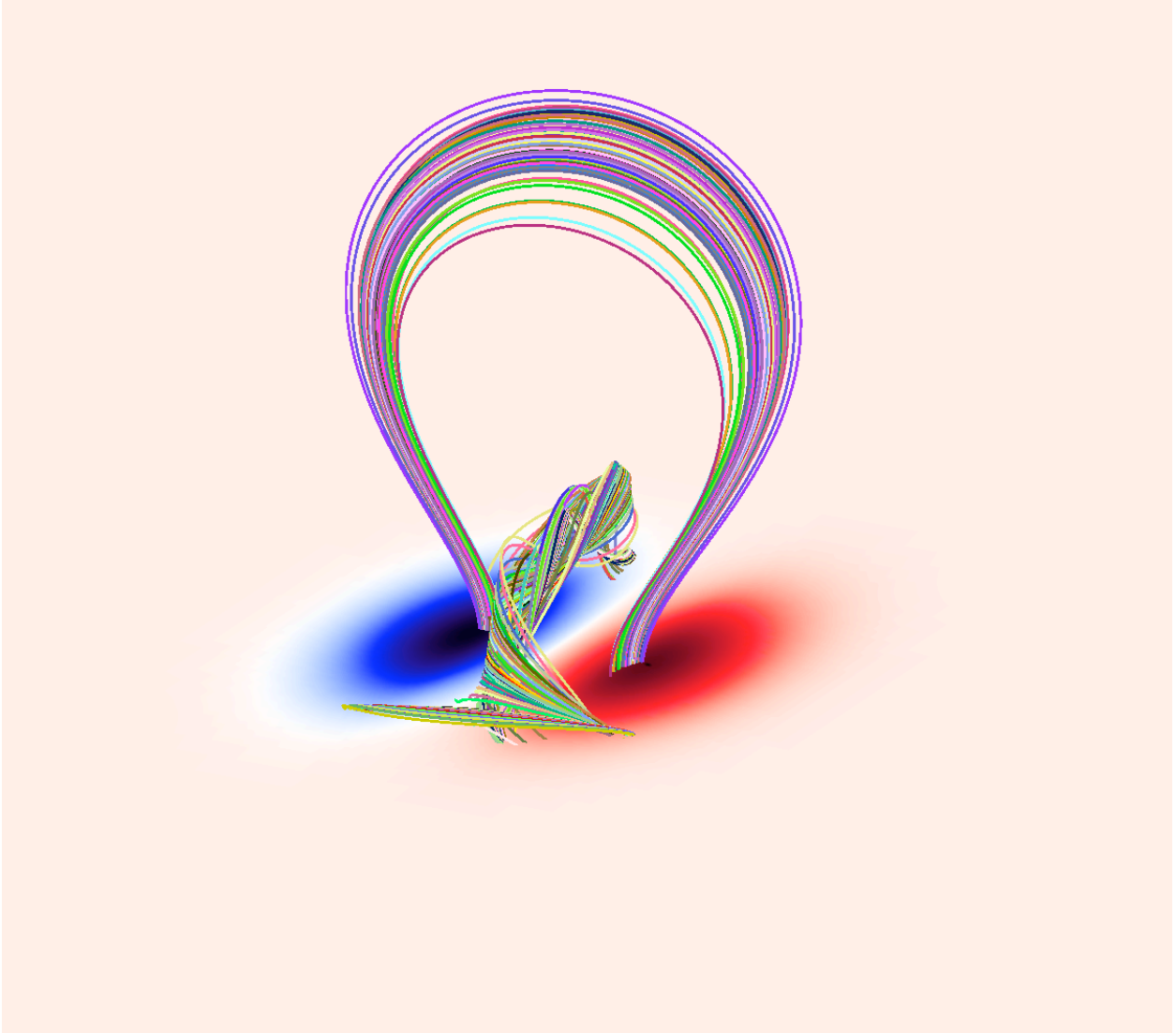


Fig. 4.— Selected field lines of the evolving configuration at  $t = 838$ , further during the phase of localised flux cancellation . Beyond this state viscous relaxation to an equilibrium does no longer hold when flux cancellation is switched off.

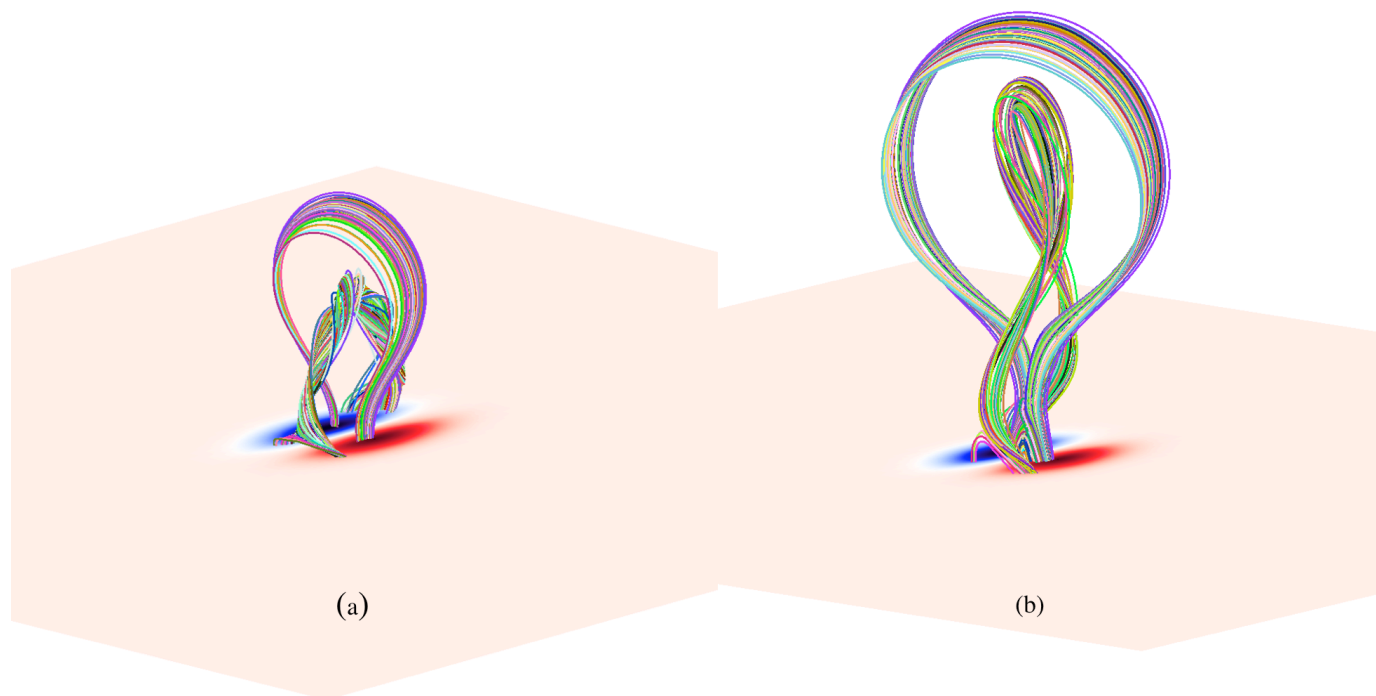


Fig. 5.— Selection of field lines of the configurations obtained at (a)  $t = 885$  and (b)  $t = 1135$  from the configuration of Figure 4, with FC switched off. The global disruption involves opening, reconnection through the overlying arcade and below, and formation of a current sheet, associated to a high dissipation of magnetic energy.